An improved deconvolution method for X-ray coded imaging in inertial confinement fusion*

Zhao Zong-Qing(赵宗清)[a)b)†], He Wei-Hua(何卫华)[a)b)], Wang Jian((王 剑)[a)b)], Hao Yi-Dan(郝轶丹)[a)b)], Cao Lei-Feng(曹磊峰)[a)b)], Gu Yu-Qiu(谷渝秋)[a)b)], and Zhang Bao-Han(张保汉)[a)b)]

[a)] *Science and Technology on Plasma Physics Laboratory, Mianyang* 621900, *China*
[b)] *Laser Fusion Research Center, China Academy of Engineering Physics, Mianyang* 621900, *China*

(Received 6 December 2012; revised manuscript received 21 February 2013)

In inertial confinement fusion (ICF), X-ray coded imaging is considered as the most potential means to diagnose the compressed core. The traditional Richardson–Lucy (RL) method has a strong ability to deblur the image where the noise follows the Poisson distribution. However, it always suffers from over-fitting and noise amplification, especially when the signal-to-noise ratio of image is relatively low. In this paper, we propose an improved deconvolution method for X-ray coded imaging. We model the image data as a set of independent Gaussian distributions and derive the iterative solution with a maximum-likelihood scheme. The experimental results on X-ray coded imaging data demonstrate that this method is superior to the RL method in terms of anti-overfitting and noise suppression.

Keywords: inertial confinement fusion, coded imaging, deconvolution, Gaussian distribution, maximum-likelihood

PACS: 42.30.Va **DOI:** 10.1088/1674-1056/22/10/104202

1. Introduction

In inertial confinement fusion (ICF), implosion core imaging is an important way to obtain the information about the symmetry, uniformity, and hydrodynamatic instability prosperities of the irradiated source.[1] As to the XingGuang-II laser facility in China, the yields of deuterium tritium (DT) neutrons and D^3He protons are quite low. However, it can produce enough X-ray for imaging. Therefore, X-ray imaging is considered as having the most potential for diagnosing the compressed core in ICF.

In conventional X-ray pinhole imaging, only a single pinhole is adopted. In this case, it is always hard to obtain an image with enough resolution to gain significant information about the compressed core. Moreover, its solid angle coverage is very small and thus it is difficult to use it for core imaging.

In the ICF field, X-ray coded imaging is a good means for compressed core imaging. Due to a large open area of aperture, which is perhaps more than 1000 times that of a single pinhole, the collect efficiency is greatly increased. Consequently, the signal-to-noise ratio (SNR) of the coded image could be sharply improved compared with the conventional pinhole imaging. This is very helpful for core imaging, especially when the X-ray has a low flux of radiation, such as in our XingGuang-II laser facility. In addition, as the object points at different distances from the aperture and casts shadows of the aperture onto the pictures with different sizes, one can even construct depth information about the particular object.[2] In a word, coded imaging is very beneficial to diagnosing the compressed core. In an early study of coded imaging, the Fresnel zone plate (FZP) is the most used coded imaging technique for α particles produced by hot electrons or X-rays emitted from the inside of the Holhraum wall in ICF.[3] At present, there exist many other kinds of image coding techniques, such as ring aperture imaging, penumbral imaging, and uniformly redundant array imaging.[2]

As the coded image is overlapped, it must be effectively deconvolved with appropriate methods. Actually, a great number of deconvolution methods have been proposed so far. Most of these methods are based on regularization by searching for best fitted models subject to the constraints such as maximum entropy and flatness.[4,5] A remarkable exception is the Richardson–Lucy (RL) iteration method, which is based on the maximum likelihood scheme.[6,7] Compared with the regularization-based methods, the RL method tends to improve the resolution of the deblurred image and is easy to implement. Thus, the RL method has received much attention and its many variants have also been proposed. For instance, Singh *et al.*[8] presented an adaptively accelerated RL method by introducing an exponent parameter into the correction ratio of the RL method. Yongpan *et al.*[9] proposed an improved RL method by introducing a spatial weight matrix as local constraint. Their method can strike a good

*Project supported by the National High-Tech ICF Committee of China, Foundation of China Academy of Engineering Physics (Grant Nos. 2009A0102003 and 2011B0102021), and the National Natural Science Foundation of China (Grant No. 10905051).

†Corresponding author. E-mail: zhaozongqing99@gmail.com

© 2013 Chinese Physical Society and IOP Publishing Ltd

balance between preserving image details and suppressing ringing artifacts. Dell'Acqua *et al.*[10] proposed a modified damped RL method to reduce isotropic background effects in spherical deconvolution. Up to now, the RL method and its variants have been widely used in many applications such as remote sensing image deconvolution,[11] fluorescence images,[12] Doppler broadening spectroscopy,[13] etc. However, the RL method still has the following disadvantages: (i) noise would be amplified with the times of iteration increasing, which makes it divergent or observably run away from a reasonable solution;[14,15] (ii) although the RL method shows the so-called object-feasibility filtering ability, it may not be well appropriate for image where the noise does not follow the Poisson distribution.

In ICF, the noise of a coded image mainly involves pulse noise by scattering particles or energetic penetrated particles, and additional noise in the system. The latter can be further classified into two categories: additive noise induced by thermal scattering and multiplicative noise by quantum gain. Usually, one system includes multiple components. The noises from these components interact, which makes them more complex. In our previous work, theoretical analysis and numerical simulations both proved that the noise in the X-ray coded image follows the Gaussian distribution.[16]

In this paper, we propose an improved deconvolving method for X-ray coded images in ICF. This method models the image data as a set of independent Gaussian distributions and derives the iterative solution with a maximum-likelihood scheme. As the priori statistical information of the Gaussian noise model has been integrated into the iteration model, the proposed method is shown to be much less sensitive to noise in our coded image, and also to be free of the over-fitting problem compared with the traditional RL method.

The rest of the paper is organized as follows. A brief review of the theory of the traditional RL method is provided in Section 2. Then, the model and basic concept of our improved method are presented in Section 3. Section 4 is devoted to the experimental results of coded-aperture imaging respectively from our improved deconvolution method and RL method, and some discussions are also made in the same section. Finally, conclusions drawn from the present study are given in Section 5.

2. RL method

The RL method, originally introduced by Richardson[6] and Lucy[7] for deblurring optical image in astrophysics, is a maximum-likelihood iterative method based on the assumption of Poisson noise distribution.

Assume that $Y_{0,i} = (H * X)_i = \sum_j H_{j-i} X_j$ is the consequence from the signal $\boldsymbol{X}$ transmitted by the point spread function (PSF) $\boldsymbol{H}$ of system, and the disturbed signals Y_i follow Poisson distribution $P(Y_i|Y_{0,i}) = (Y_{0,i}^{Y_i}/Y_i!)\exp(-Y_{0,i})$ with parameter $Y_{0,i}$ for each pixel i.

The maximum-likelihood method is employed to estimate the solution $\hat{\boldsymbol{X}}$ by maximizing the likelihood function $L[\boldsymbol{X}] = \sum_i \ln P(Y_i|Y_{0,i})$.

The basic iteration formula for the RL method is

$$\hat{\boldsymbol{X}}^{(n+1)} = \hat{\boldsymbol{X}}^{(n)} \cdot \left(\boldsymbol{H}^R * \frac{\boldsymbol{Y}}{\boldsymbol{H} * \hat{\boldsymbol{X}}^{(n)}} \right), \tag{1}$$

where the superscript R denotes the reversal of array in each dimension, the symbol $*$ the convolution, and the dot "$\cdot$" the point-wise multiplication.

3. Proposed improved deconvolution method

In the ICF method, the coded imaging process includes two steps. The first step is to generate the coded image, in which a geometrical shadow is cast on the charge-coupled device (CCD) detector through a large ring aperture irradiated by X-ray. This image formation process can be written as

$$\boldsymbol{Y} = \boldsymbol{H}\boldsymbol{X} + \boldsymbol{\eta}, \tag{2}$$

where $\boldsymbol{Y}$ is the intensity of the degraded image in the detector plane, $\boldsymbol{X}$ the spatial distribution in the source plane, $\boldsymbol{H}$ the transmission of the aperture in the aperture plane (i.e., the system's PSF), and $\boldsymbol{\eta}$ the zero mean Gaussian noise, with variance σ.

The second step is to restore the original source distribution from the coded image with the deconvolution technique. In the following, we will show how to restore the coded image using the proposed improved deconvolution method.

According to Eq. (2), the conditional probability of $Y_k\,(k = 1,\ldots,N)$ can be expressed as follows:

$$p(Y_k|X_k) = \frac{1}{\sqrt{2\pi}\sigma} \exp\left\{ -\frac{1}{2} \left[\frac{Y_k - (HX)_k}{\sigma} \right]^2 \right\}. \tag{3}$$

The corresponding joint log-likelihood function is then

$$\begin{aligned} L(\boldsymbol{X}) &= \ln \prod_{k=1}^{N} p(Y_k|X_k), \\ &= -\frac{1}{2\sigma^2} \sum_{k=1}^{N} [(Y_k - (HX)_k)^2] - \frac{N}{2} \ln \sigma^2 - \frac{N}{2} \ln (2\pi) \\ &= -\frac{1}{2\sigma^2} \sum_{k=1}^{N} [(Y_k - (HX)_k)^2] + c, \end{aligned} \tag{4}$$

where constant

$$c = -\frac{N}{2} \ln \sigma^2 - \frac{N}{2} \ln (2\pi)$$

represents the term independent of I_i.

The maximum likelihood solution occurs where all the partial derivatives of $L(\boldsymbol{X})$ with respect to X_j, i.e.,

$$\begin{aligned}\frac{\partial L}{\partial X_j} &= \partial_{X_j}\left[-\frac{1}{2\sigma^2}\sum_{k=1}^{N}(Y_k-(HX)_k)^2+c\right]\\ &= -\frac{1}{2\sigma^2}\partial_{X_j}\left[\sum_{k=1}^{N}\left(Y_k-\left(\sum_{i=1}^{N}H_{ki}X_i\right)\right)^2\right]\\ &= -\frac{1}{2\sigma^2}\left[\sum_{k=1}^{N}\left(-2H_{kj}Y_k+2H_{kj}\left(\sum_{i=1}^{N}H_{ki}X_i\right)\right)\right]\\ &= \frac{1}{\sigma^2}\left[\sum_{k=1}^{N}\left(H_{kj}\left(\sum_{i=1}^{N}H_{ki}X_i\right)-H_{kj}Y_k\right)\right] \qquad (5)\end{aligned}$$

are equal to zero.

According to Eq. (5), we can derive the iterative scheme

$$\hat{X}_j^{(n+1)} = \hat{X}_j^{(n)}\frac{\sum_{k=1}^{N}H_{kj}Y_k}{\sum_{k=1}^{N}H_{kj}\left(\sum_{i=1}^{N}H_{ki}\hat{X}_i^n\right)}. \qquad (6)$$

As for the linear system, the PSF $\boldsymbol{H}$ is spatially invariant. Then Eq. (6) can be rewritten in the following convolution form:

$$\hat{X}_j^{(n+1)} = \hat{X}_j^{(n)}\cdot\frac{\boldsymbol{H}^R * \boldsymbol{Y}}{\boldsymbol{H}^R * \left(\boldsymbol{H} * \hat{X}_i^n\right)}. \qquad (7)$$

4. Experimental results and discussion

It is an important job to study the interaction between a laser and a target and measure the characteristics of an X-ray in ICF, such as photon yield, energy spectrum, and source size. In this section, we use the proposed method and the traditional RL method to restore the source information of coded images taken from the XingGuang-II laser facility and the SILEX facility, respectively. The comparison results and analyses are given in the same section.

The illustration of the experimental set at the XingGuang-II laser facility is shown in Fig. 1. Irradiated by a 700-ps pulse laser with different energy values, the Ti bulk solid target produces $K\alpha$ line of Ti. The ring aperture is coated with Au with a thickness of 10 μm, and its annulus width and external diameter are 5 μm and 1000 μm, respectively. There is also a pinhole in the center of the ring aperture, whose diameter is 5 μm. The CCD detector is used to record the X-ray coded image and the pinhole image at the same time. As the pinhole image can directly show a rough shape of the source, it will be convenient for us to qualitatively verify the deconvolution result of the coded image.[1]

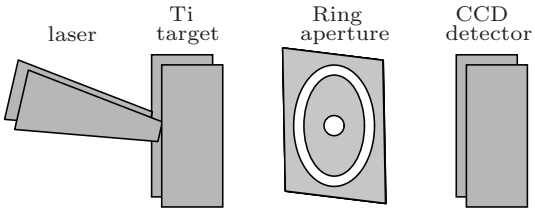


Fig. 1. Illustration of the ring aperture imaging experiment.

Figure 2(a) shows an X-ray coded image, and in its center is the pinhole image. Detailed information about this pinhole image is shown in Fig. 2(b).

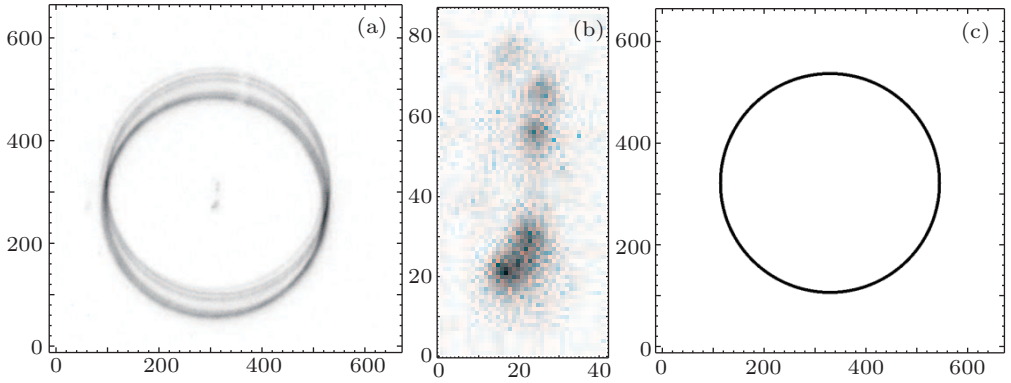


Fig. 2. The X-ray coded image and the corresponding PSF: (a) coded image, (b) pinhole image, (c) corresponding PSF. The unit for x and y axes is pixel, which is usually omitted in the figures.

It should be noted that in the image deblurring process, the pinhole image centred at the coded image must be removed to avoid its influence on deconvolution results. An ideal PSF is employed, which is a ring with 211 pixels of inner radius and 6 pixels of ring width (Fig. 2(c)). The deblurred results of the coded image Y by RL with 50, 500, 2000, 3000, and 5000 iteration times are shown in Figs. 3(a)–3(e), while the deblurred results by our method are shown in Figs. 4(a)–4(e). It can be seen that the traditional RL method achieves the best result after about 500 iteration times (the best result is determined by searching for the minimum variance of the difference between the original coded image and the generated convolved

image). However as the iteration times further increase, the deblurred images by RL turn worse due to its over-fitting. On the contrary, the deblurred results by our method are all gradually improved through the iteration process.

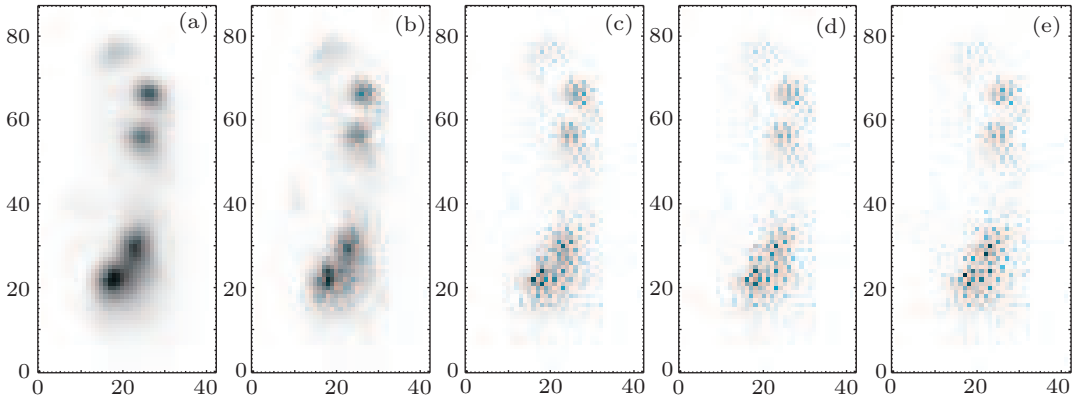


Fig. 3. Deblurred results by the traditional RL method with different iteration times: (a) 50, (b) 500, (c) 2000, (d) 3000, and (e) 5000 iteration times.

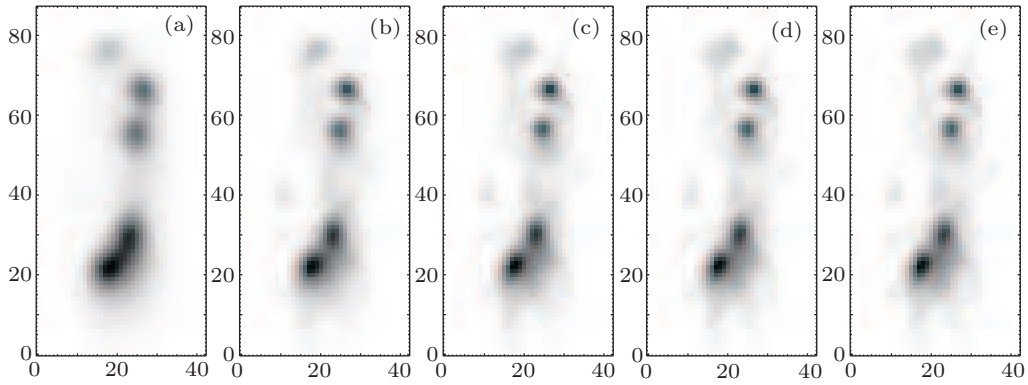


Fig. 4. Deblurred results by our proposed method with different iteration times: (a) 50, (b) 500, (c) 2000, (d) 3000, and (e) 5000 iterations.

Figure 5 shows the pinhole image and the best deblurred images by the traditional RL method and our method, respectively. From it we can find that i) the results by the RL method and our method are in good agreement with those obtained by the pinhole imaging; ii) the deblurred image by our method has the highest resolution, while the pinhole has the lowest resolution.

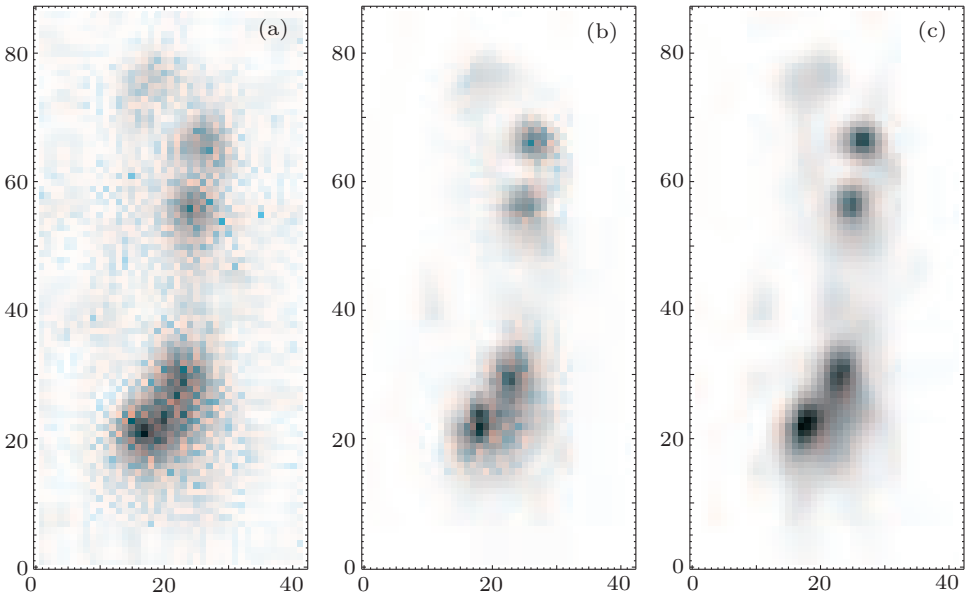


Fig. 5. The best deblurred results by the RL method and our method, as well as the pinhole image: (a) pinhole image, (b) best of RL, (c) best of ours.

To verify the noise distribution of the X-ray coded image, the best deblurred result by our method is chosen and then convoluted by the PSF $\boldsymbol{H}$. The noise can be estimated by subtracting the resulting convoluted image from the original coded image, which is shown in Fig. 6(a). The resulting noise distribution is shown in Fig. 6(b). For comparison, the Gaussian distribution is shown in the same figure. It can be seen that the noise of coded image approximately follows the Gaussian distribution.

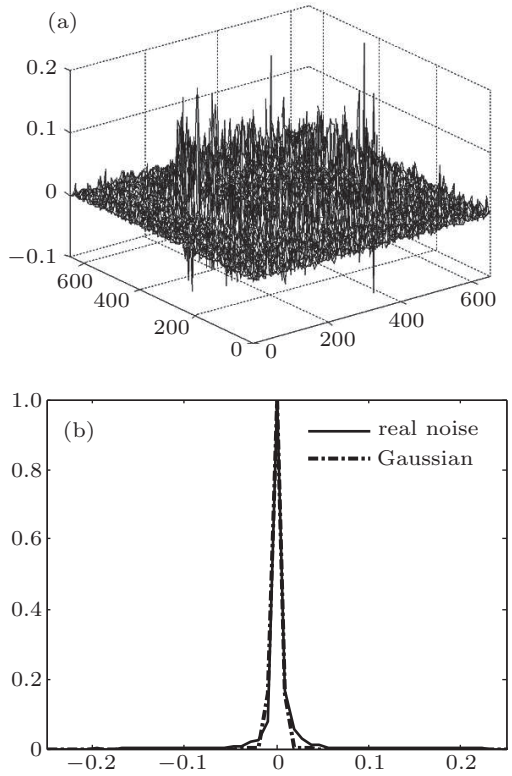


Fig. 6. Comparison of the noise distribution of the coded image with Gaussion distribution: (a) estimated noise of the coded image, (b) comparison of noise distribution.

Subsequently, we measure the fitnesses of the methods according to the variance of the difference between the original coded image and the generated convolved image (herein the convolved image is generated by the convolving the deblurred result with the PSF), which is defined as

$$\Delta V^{(t)} \stackrel{\text{def}}{=} \text{var}(\boldsymbol{Y} - \boldsymbol{H} * \boldsymbol{X}^{(t)}).$$

The variances in the whole iteration process for the two methods are shown in Fig. 7. The fitness value of the RL method reaches its minimum after about 500 iterations, and then turns worse as the iteration time increases. However, our method keeps improving the fitness as the iteration time increases. Evidently, this result is well consistent with the conclusion observed in Fig. 3.

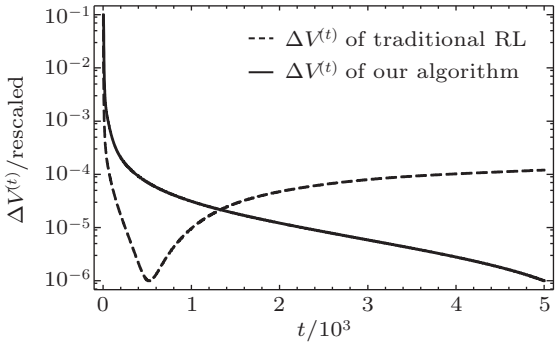


Fig. 7. Fitnesses of RL and our proposed method.

To validate its robustness to the shape of code aperture, we also restore the penumbral-aperture image from the SILEX facility with our method. Different from the ring aperture in the XingGuang-II laser facility, a circle aperture with a diameter of 800 μm is employed as the coded aperture. A photon X-ray CCD detector is used to collect the coded image. To obtain the source size, the traditional RL method and our method are both employed to restore the penumbral image. Figure 8 shows the best deblurred results by the two methods. From this figure, it can be seen that due to the low signal-to-noise ratio of the penumbral image, the RL method gives an overfitted result. On the contrary, our method gives a good restored image with a clear source structure and detail, which indicates that our method not only has a better ability to prevent overfitting and noise suppression, but also has good robustness to the shape of the code aperture.

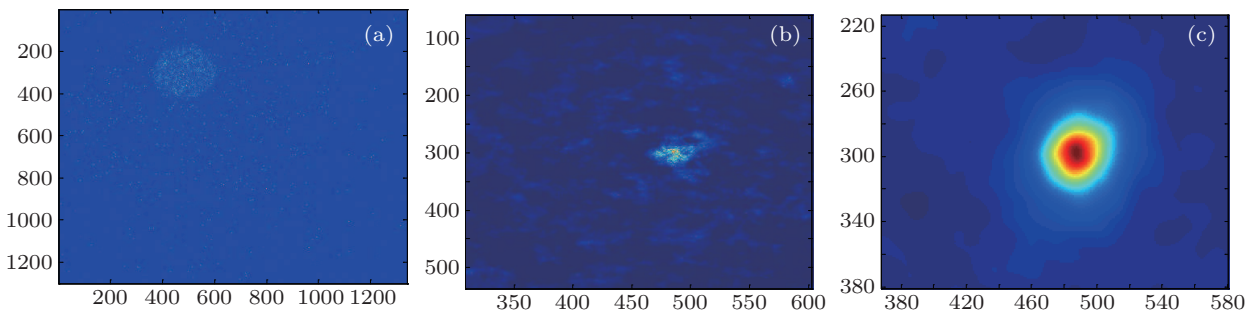


Fig. 8. (color online) The best deblurred results of the RL method and our method: (a) penumbral image, (b) best of RL, (c) our method.

5. Conclusions

X-ray coded imaging is considered as the most promising means to diagnose the compressed core in ICF. In this paper, we propose an improved deconvolution algorithm for X-ray coded imaging. We model the image data as a set of independent Gaussian distributions and derive the iterative solution with maximum-likelihood scheme. With the XingGuang-II laser facility, we conduct the X-ray ring-aperture coded imaging experiment and deconvolute the coded images with our method and the RL method, respectively. In addition, we report on the comparison result of deblurred image from the SILEX facility by using the two methods. The experimental results show that the deblurred image with our method has better resolution than the pinhole image; and our method is superior to the RL method in terms of noise suppression, anti-overfitting and robustness to the shape of code aperture.

In this paper, a ring aperture and a penumbral aperture are used for X-ray coded imaging. In future, we will also design other types of coded apertures, such as the uniformly redundant array, to further improve the SNR and resolution for low-intensity sources (particularly relevant to the X-ray imaging). In addition, the object will cast different shadows on the CCD detector according to its depth information and supply some computerized tomography (CT) resolution.[3] We will focus on reconstructing the three-dimensional object by effectively exploiting the depth information contained in the coded image.

References

[1] Zhao Z Q, Ding Y K, Dong J J, Hao Y D, Wu S C, Cao L F and Pu Y K 2007 *Plasma Physics and Controlled Fusion* **49** 1145
[2] Fenimore E E and Cannon T 1978 *Appl. Opt.* **17** 337
[3] Jiang S E, Cao L F, Yu Y N, Li C G and Zheng Z J 2004 *Physics* **33** 677 (in Chinese)
[4] Cornwell T and Evans K 1985 *Astron. Astrophys.* **143** 77
[5] Gosselin K R and Renfro M W 2012 *Appl. Opt.* **51** 1671
[6] Richardson W H 1972 *JOSA* **62** 55
[7] Lucy L 1974 *AJ* **79** 745
[8] Singh M K, Tiwary U S and Kim Y H 2008 *EURASIP Journal on Advances in Signal Processing* **2008** 52
[9] Wang Y P, Feng H J, Xu Z H, Li Q and Dai C Y 2010 *Optics & Laser Technology* **42** 845
[10] Dell'Acqua F, Scifo P, Rizzo G, Catani M, Simmons A, Scotti G and Fazio F 2010 *Neuroimage* **49** 1446
[11] Dong W, Feng H, Xu Z and Li Q 2011 *Optics & Laser Technology* **43** 926
[12] Zhang H, Zhang Z, Luo Q and Zeng S 2007 *Biomedical Optics* 64360P
[13] Zhang J, Zhou T, Cheung C, Beling C, Fung S and Ng M 2006 *Nuclear Instruments and Methods in Physics Research Section A: Accelerators, Spectrometers, Detectors and Associated Equipment* **560** 552
[14] Bi H and Boerner G 1994 arXiv: astro-ph/9409093.
[15] Bratsolis E and Sigelle M 2001 *Astron. Astrophys.* **375** 1120
[16] Zhao Z 2008 "Numerical Simulation and Optimization Design of Neutron Penumbral Imaging Technology in Laser Fusion Research", Ph. D. Thesis (Beijing: Tsinghua University) (in Chinese)